Measurement of Pulsation Strain at the Fingertip Using a Plastic FBG Sensor

Shouhei Koyama, *Member, IEEE*, Yuki Haseda, Hiroaki Ishizawa, *Member, IEEE*, Futa Okazaki, Julien Bonefacino, and Hwa-Yaw Tam, *Fellow, IEEE*

***Abstract*— There is a need to develop sensors that can measure vital signs such as pulse rate and blood pressure easily; such vital signs can be calculated by measuring arterial strain. To this end, a new method that uses a plastic fiber Bragg grating (FBG) sensor to measure pulsation strain at human fingertips is proposed herein. Plastic fiber has a smaller Young's modulus than that of the glass fiber. Under the same applied pressure, the plastic FBG sensor deforms more than the silica glass FBG sensor, and the Bragg wavelength shift length becomes longer, which results in higher detection sensitivity. The pulsation strain of the fingertip was measured by the proposed method based on this characteristic. The most sensitive signal detection point in the fingertip was the measurement point 10 or 15 mm from the distal interphalangeal joint in the fingertip direction. Strain signals with periodic peaks were measured from five participants. From the strain signal measured with the cuff attached to the arm, the peak disappeared when the cuff moved, and it reappeared when the cuff was opened. Therefore, the measured signal waveform changes based on the blood flow condition. The pulse rate calculated from the peak interval of the measured signal showed high correlation with the reference pulse rate, and the measurement accuracy was ±5.5 bpm. It may be possible to calculate the blood pressure and pulse rate from the measurement signal of the pulsation strain of the fingertip obtained using the plastic FBG sensor.**

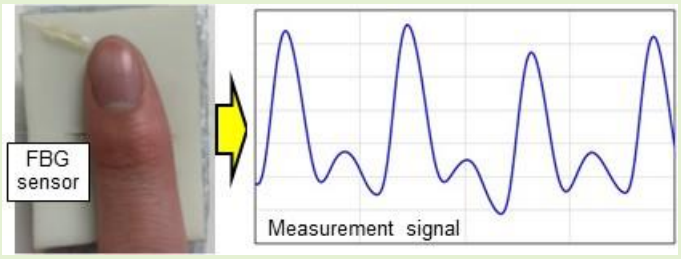

***Index Terms*— Plastic optical fiber, Fiber Bragg grating sensor, Pulsation strain, Fingertip, Pulse wave signals, Pulse rate.**

I. Introduction

VITAL signs include pulse rate, respiratory rate, blood pressure, and body temperature. In recent years, owing to the growing awareness of human health metrics, sensors that can measure vital signs quickly and unobtrusively have gained considerable attention. A photoplethysmography (PPG) sensor is a typical wearable sensor; the measurement principle of this sensor was proposed by Hertzman in the 1930s [1]. There are two main types of PPG sensor: one that uses a green light-emitting diode (approximately 500-550 nm [2-4] and the other that uses a near-infrared light source (approximately 600-1,300 nm) [5-6]. The difference in the light-source wavelength affects the photonic penetration depth in a living body [7]. The light of each source is absorbed by the hemoglobin inside the capillaries, and it reappears outside the living body, which allows its detection. The amount of hemoglobin in the capillaries changes as the heart contracts, and therefore, the signal strength corresponding to that amount can be detected [8]. The measured signal intensity changes are related to the contraction of the heart, which can be calculated by detecting the peak intensity of the measured signal; further, it can be correlated to the pulse rate. The amount of hemoglobin is maximized when the heart contracts, and the measurement signal is detected during contraction as the bottom peak. The positive features of the PPG sensor include its small size, low power consumption, and long life. Further, because capillaries are present in all body surfaces, the devices can be attached anywhere. Signals with high signal-to-noise (S/N) ratios can be measured at the fingertips and ear lobes where the capillaries are highly concentrated. However, if there is a gap in space between the sensor and the living body, the light will scatter, and the S/N ratio of the detection signal will drop significantly.

This research was partially supported by the Creation of a development platform for implantable/wearable medical devices by a novel physiological data integration system of the Program on Open Innovation Platform with Enterprises, Research Institute and Academia (OPERA) from the Japan Science and Technology Agency (JST) Grant Number JPMJOP1722. This work was also supported by JSPS KAKENHI Grant Number JP16H01805.

All participants gave their informed consent for inclusion before they participated in the study. The study was conducted in accordance with the Declaration of Helsinki, and the protocol was approved by the Ethics Committee of Shinshu University (No. 3202, Verification clinical trial with wearable vital sign measurement system.).

Shouhei Koyama and Fuuta Okazaki are with the Faculty of Textile Science and Technology, Shinshu University, 3-15-1, Tokida, Ueda-city, Nagano, Japan (e-mail: shouhei@shinshu-u.ac.jp, 17f1011h@shinshu-u.ac.jp).

Yuki Haseda is with the Graduate School of Science and Technology, Shinshu University, 3-15-1, Tokida, Ueda-City, Nagano, Japan (e-mail: 19hs115f@shinshu-u.ac.jp).

Shouhei Koyama and Hiroaki Ishizawa are with the Institute for Fiber Engineering, Shinshu University, 3-15-1, Tokida, Ueda-City, Nagano, Japan (e-mail: shouhei@shinshu-u.ac.jp, zawa@shinshu-u.ac.jp).

Julien Bonefacino and Hwa-Yaw Tam are with the Department of Electrical Engineering, Photonics Research Centre, The Hong Kong Polytechnic University, 11 Yuk Choi Road, Hung Hom, Kowloon, Hong Kong, China (e-mail: jeebonef@polyu.edu.hk, hwa-yaw.tam@polyu.edu.hk).

Therefore, the device must remain in close contact with the skin. In addition, the signal waveform is considerably disturbed by motion during exercise, and research is underway to develop method to mitigate this problem [9-12].

There is another approach for measuring the strain of arteries and calculate the vital signs. Tonometry – a blood pressure measurement method - is a typical example of a pulsation strain measurement. When the pulsation strain is measured, vital signs such as pulse rate or blood pressure are calculated. A fiber Bragg grating (FBG) sensor is an optical fiber high-sensitivity strain sensor. In a previous study, a silica glass FBG sensor was installed at the pulsation points of the wrist or elbow of a participant to measure the strain of the pulsation point. In the experiment, the signal measured by the FBG sensor showed changes in fluid pressure [13] and arterial diameter [14]. The pulse rate, stress, respiratory rate, blood pressure, etc. were calculated based on these measured signals [15-19]; thus, pulsation strain can be employed to detect multiple biological variables. The silica glass FBG sensor needs to be installed at a pulsation point where the pulsation strain can be detected with human fingertips. The pulsation points on the surface of the living body that can be detected by human touch are limited to the elbows, wrists, neck, and ankles, which is a drawback of conducting measurements with FBG sensors.

The heart pumps blood throughout the body using arteries, and therefore, it is assumed that small pulsation strains occur throughout the body. However, a more sensitive strain sensor than the FBG sensor is required to detect these small strains. To this end, an FBG sensors made of plastic fiber, which has a smaller Young's modulus than that of the glass fiber [20] is employed. Under the same applied pressure, plastic fiber shows a higher deformation than that of the glass fiber. For the FBG sensor, the greater the deformation of the fiber, the longer the shift length of the Bragg wavelength, and thus, the strain is detected with a higher sensitivity [21]. In other words, plastic FBG sensors are more sensitive than silica glass FBG sensors, and therefore, they have an advantage in that they can be applied at more places to measure the pulsation strain compared to that using FBG sensors.

The fingertip was selected as the measurement point for the plastic FBG sensor because capillaries are concentrated in the fingertips, and the arteries are also present, which results in pulsation strains. Fingertips are separated from the trunk, which gives the participant a sense of safety. In addition, this sensor can be used to perform measurements on anyone (from children to the elderly).

In this study, a plastic FBG sensor system that can measure pulsation strain of fingertips is introduced. The installation conditions and positions for measuring the pulsation strain at the fingertips with high sensitivity are verified. A cuff was installed on the forearm, and the measurement signal waveform when the blood flow condition changed because of the movement of the cuff was measured. Further, from this signal waveform, the effect of blood flow status was verified. Moreover, the pulse rate was calculated from the signal measured, and its measurement accuracy was verified.

The remainder of the paper is divided as follows. Measurement principle and specification of the plastic FBG sensor system are presented in Section II. Each experiment and result are presented in Section III (Section III-A: Verification of optimal measurement condition for pulsation strain at the fingertip, Section III-B: Measurement signal waveform at the fingertip when blood flow changes, Section III-C: Calculation of pulse rate with a plastic FBG sensor system). Conclusions and future works are depicted in Section IV.

II. Plastic FBG Sensor System

The measurement sensor system comprises an FBG interrogator and a measurement attachment with an plastic FBG sensor. The diagram of the sensor system is shown in Fig. 1(a). Table I lists the specifications of the FBG interrogator, which is a wavelength-division multiplexing type (Kyowa Electronic Instruments Co., Ltd., EFOX-1000B-4).

Two types of optical fibers (i.e., silica glass (1 m) and plastic (50 mm)) were used as sensors. The plastic fiber was in single mode type and had a core diameter of 5.5 μm. Since the core

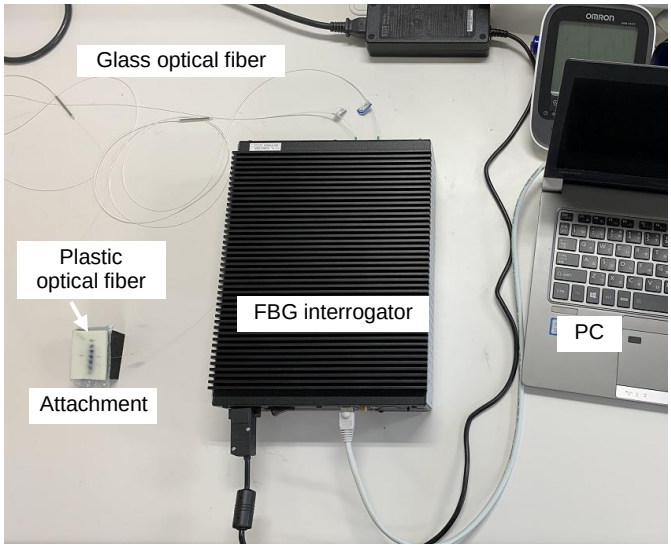

(a)

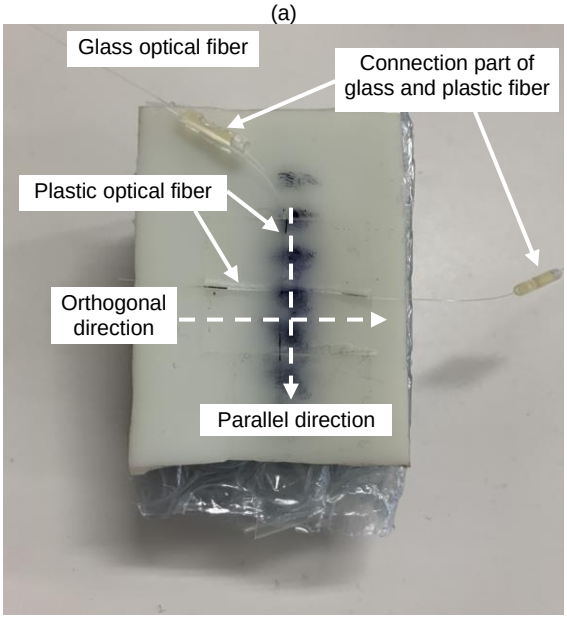

(b)

Fig. 1. Plastic FBG: (a) sensor system; (b) measurement attachment

TABLE I
SPECIFICATIONS OF THE FBG INTERROGATOR AND THE FBG SENSOR

FBG interrogator		
Scan frequency (Hz)		1,000
Wavelength range (nm)		1,460-1,620
Accuracy (pm)		Within ±1
Dynamic range (dB)		25
FBG sensor		
Glass optical fiber	Material	Silica glass
	Length (mm)	1,000
	Fiber diameter (μm)	125
	Core diameter (μm)	8
Plastic optical fiber	Material	PMMA
	Length (mm)	50
	Fiber diameter (μm)	120
	Core diameter (μm)	5.5
	FBG sensor length (μm)	10
	Bragg wavelength (μm)	1,550

diameter was thin, the intensity of the incident infrared light was very low. Further, the propagation loss was large, and the plastic fiber could not be lengthened. An optical fiber made of silica glass was used to connect the plastic fiber and the FBG interrogator. The cross section of the glass optical fiber was cleaved at an angle of 8° to avoid Fresnel reflections. These fibers were connected using an ultraviolet-curable adhesive (Norland Products Inc., NOA 78). The glass optical fiber had a diameter of 125 μm and a core diameter of 8 μm. The plastic optical fibers were manufactured at the Hong Kong Polytechnic University using polymethylmethacrylate (PMMA) with a diameter of 120 μm and core diameter of 5.5 μm [22]. The FBG sensor was inscribed in a 10-mm-long PMMA fiber. The effective refractive index of the PMMA fiber core was 1.488@632 nm. The plastic FBG sensor was inscribed using a He-Cd laser (KIMMON, IK3501R-G, 325 nm) and a phase mask (Ibsen, 1046.3 nm pitch) [22]. The S/N ratio of this FBG sensor was approximately 25 dB. Plastic optical fiber have a large optical loss rate, and they cannot propagate infrared light over a long distance. Therefore, infrared light was propagated using the glass optical fiber, and the plastic fiber was used for only the sensor.

A ferrule connector/angle physical contact (FC/APC) connector was installed on the end face of the glass optical fiber and connected to the FBG interrogator. The near-infrared light emitted from the broadband near-infrared light source in the FBG interrogator passed through the glass optical fiber and reached the FBG sensor in the plastic optical fiber. The FBG sensor was used to reflect only the near-infrared light at the Bragg wavelength; other wavelengths were transmitted. The reflected Bragg wavelength was detected by a detector inside the FBG interrogator. The Bragg wavelength was calculated using

$$\lambda_{Bragg} = 2n_{eff}\Lambda \quad (1)$$

where λ_{Bragg}, Λ and n_{eff} denote the Bragg wavelength, periodic length of the refractive index change forming the FBG sensor, and effective refractive index in the core of the optical fiber. respectively. Further from Equation 1, the Bragg wavelength can be calculated by the periodic length of the refractive index change that forms the FBG sensor because n_{eff} is constant. This periodic length changes when the optical fiber expands and contracts as the strain is applied to the sensor. Thus, the detected Bragg wavelength also changes. The strain applied to the FBG sensor can be detected by the change in Bragg wavelength. Because the Young's modulus of the PMMA fiber is small, the fiber is greatly deformed, and therefore, the shift length of the Bragg wavelength becomes long and the strain detection sensitivity improves.

An installation attachment (Fig. 1(b)) was created using a 3D printer to make it easier to install the FBG sensor on the fingertips. The size of this attachment is 40 × 50 × 10 mm, and the material is poly-lactic-acid. A 3-mm-thick gel sheet is placed on the surface of this attachment to prevent the plastic optical fiber from being crushed when the fingertip is pressed against the FBG sensor. The sampling rate of the sensor is 1,000 Hz. Because the measured signal contains noise, the signal processed via bandpass filtering (BPF) at 0.5–5 Hz becomes the measured signal waveform. Using this BPF processing, the vertical axis of the measurement signal shows only the shift length of the Bragg wavelength caused by the pulsation strain.

III. METHODS AND RESULTS

A. Verification of optimal measurement condition for pulsation strain at the fingertip

The installation conditions of the plastic FBG sensor must be verified to measure signals with high S/N ratios. The FBG sensor is an optical fiber with a linear shape. The measurement signal changes depending on whether it is installed parallel or orthogonal to the finger direction. Therefore, as shown in Fig. 2(a), two plastic FBG sensors are installed on the measurement attachment parallel and orthogonal to the finger direction. The fingertip is pressed onto the crossed FBG sensor, and the pulsation strain signal is measured using the two FBG sensors. Subsequently, the optimum installation position of the FBG sensor in the fingertip is verified. Fig. 2(b) shows that the measurement points contain four parts with lengths 5, 10, 15, and 20 mm in the fingertip direction from the distal interphalangeal (DIP) joint. First, the pulsation strain signal is measured by pressing a point 5 mm from the DIP joint against the FBG sensor. Next, the fingertip is separated from the FBG sensor. Then, a point 10 mm from the DIP joint is pressed against the FBG sensor, and the pulsation strain signal is measured. Similarly, signals are measured at points 15 mm and 20 mm from the DIP joint. The pulsation strain is measured three times at each part. The vertical axis values of the peaks' tops and bottoms are then detected and averaged. The absolute value of the average value of the peak top and that of the peak bottom are added to provide the amplitude length as a single measurement signal. This amplitude length is calculated three times for each participant, and the average value is defined as the average amplitude length. The optimum FBG sensor installation direction and measurement part are verified using the calculated average amplitude length. A total of five participants participates in these experiments.

Fig. 3(a) presents the signals measured at the 10-and 20-mm points for participant C using the FBG sensor installed orthogonally to the finger direction. A periodic signal appears in the signal measured in the 10 mm part shown in Fig. 3(a).

(a)

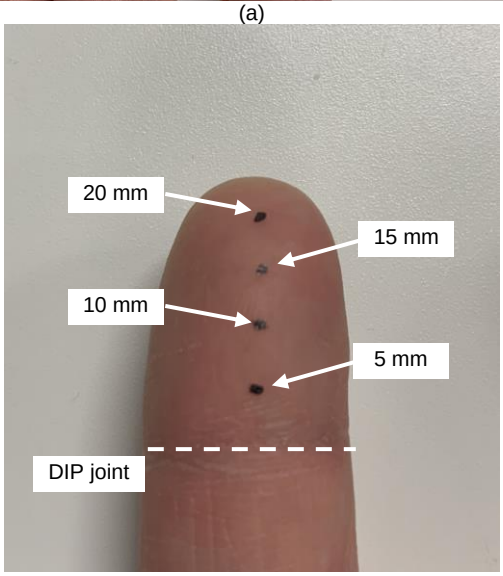

(b)

Fig. 2. Photograph of the measurement when the fingertip is pressed against the attachment where two FBG sensors are installed: ((a) A state wherein the fingertip is pressed against an FBG sensor installed parallel and orthogonal to the finger direction; (b) Four measuring points with lengths 5 mm, 10 mm, 15 mm, and 20 mm in the fingertip direction from the distal interphalangeal joint.)

The top peak of this signal was approximately 0.06, the bottom peak was approximately -0.02, and the average amplitude length was 0.083. Because the periodic signal was measured, the strain caused by the pulsation of the fingertip was expected to be detected. However, in the signal measured in the 20 mm part shown in Fig. 3(a), no periodic signal was detected, and the amplitude value was ± 0.02, which was shorter than that of 10 mm signal. When a periodic signal cannot be detected as shown in 20 mm signal, it is defined as "NG." Table II lists the average amplitude length calculated from the signal waveform measured by the FBG sensor installed in the direction parallel or orthogonal to the finger direction at each part of the five participants.

Each value lists in Table II represents the average value of the signals measured three times at the same measurement point under the same conditions. No participant can measure the strain signal at all four points from the DIP joint to the fingertip direction at 5, 10, 15, and 20 mm. Therefore, there are some

TABLE II
AVERAGE AMPLITUDE LENGTH FOR EACH PARTICIPANT MEASURED BY TWO FBG SENSORS AT FOUR MEASUREMENT POINTS

Participant	Direction	5 mm	10 mm	15 mm	20 mm
A	Parallel	NG	0.296	0.141	NG
	Orthogonal	NG	0.259	0.139	NG
B	Parallel	NG	0.079	0.048	0.085
	Orthogonal	NG	0.026	0.058	0.107
C	Parallel	0.071	0.095	0.080	NG
	Orthogonal	0.073	0.083	0.065	NG
D	Parallel	NG	0.070	0.087	NG
	Orthogonal	NG	0.055	0.055	NG
E	Parallel	NG	0.059	0.108	0.162
	Orthogonal	NG	0.118	0.179	0.137

points on the fingertip where the strain can be measured, and there are some points where it cannot be measured. Further, many participants cannot present the required strain at the 5- and 20-mm measurement points. Even when they can, only one measurement point tends to be available. Strain signals were measured at points 10 and 15 mm in all five participants. These measurement points were located 10 mm or more from the DIP joint of the finger, and they were flat parts that presented sparse unevenness on the distal phalanx. At these measurement points, the FBG sensor was expected to be in a state where it is easy to measure the strain without moving the fingertips. The length from the DIP joint to the fingertips in the five participants was approximately 20–25 mm. Therefore, in the strain measurement at the fingertip, the central part of the distal phalanx was found to be the most suitable measurement point.

For the installation direction of the FBG sensor, no significant difference was observed between the direction parallel and orthogonal to the finger directions. Participants A, C (Fig. 3(b)), and D had longer average amplitude lengths in the parallel direction, and participants B and E (Fig. 3(c)) had longer average amplitude lengths in the orthogonal direction. Thus, the results differed for each participant in the installation direction. In terms of the angle at which the FBG sensor was installed with respect to the direction of the fluid in the previous study, a signal with a higher S/N ratio was measured in the orthogonal direction [13]. No such phenomenon was observed in the fingertip measurements, and this was attributed to be the direction of the artery at the fingertip. These arteries formed a transverse palmar arch with a diameter of about 0.8 mm near the DIP joint [23]. From this arch, the artery became a narrower blood vessel with a diameter of approximately 0.6 mm and progressed to the entire fingertip in a random direction. Therefore, the arterial direction of the measured part was not a straight line with respect to the finger direction. Further, there is no significant difference in the measurement signals even when the FBG sensor is installed in different directions. In addition, Hattori et al. reported that this narrow blood vessel is located in the center of the volar side of the distal phalanx [24], and it is consistent with the location at which the strain is measured in this experiment. Based on this information, the strain signal detected by the FBG sensor well-measured the strain created in

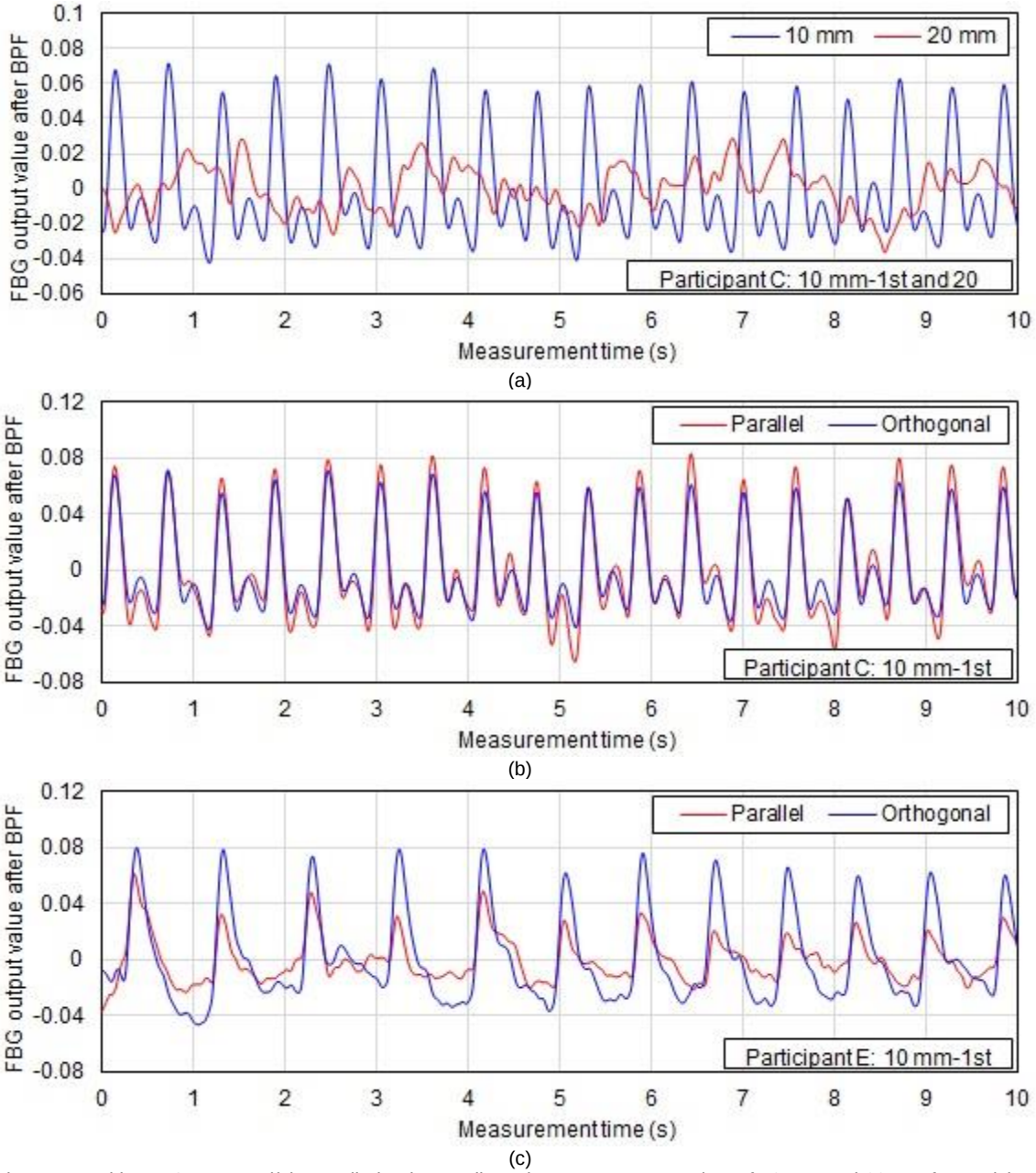

Fig. 3. Signals measured by FBG sensors ((a): Installed orthogonally at the measurement points of 10 mm and 20 mm for participant C (1st time measurement), (b): Installed parallelly and orthogonally at the measurement point of 10 mm for participant C (1st time measurement), (c): Installed parallelly and orthogonally at the measurement point of 10 mm for participant E (1st time measurement).

the narrow artery at the tip of the DIP joint.

B. Measurement signal waveform at the fingertip when blood flow changes

The relationship between the signal measured by the FBG sensor and the pulsation strain caused by the blood flow was verified. The FBG sensor measured some strain at the fingertip, which was then predicted to be a pulsation strain caused by blood flow. Thus, the measured signal waveform that occurred when the pulsation strain was intentionally changed was verified. The pulsation strain of the fingertip was measured at the optimum installation direction, and the optimum measurement part of the plastic FBG sensor was illustrated in the abovementioned experiment. A cuff-type electronic sphygmomanometer (Omron Corp., HEM-7511T) was installed on the forearm to control the blood flow. When this cuff was operated, the forearm was tightened, and blood did not flow from the forearm to the fingertips. Thus, it is predicted that the measurement signal waveform would be affected by the change in the blood-flow condition at the fingertips. A fingertip was then placed on the plastic FBG sensor, and the pulsation strain signal was measured for 5 s. Then, a cuff-type electronic sphygmomanometer was used. While the cuff was operated, the participant was asked to declare the tightening state of the cuff (eg, “Cuff pressure is applied.”, “Cuff pressure is decreasing.”, “Cuff pressure is nothing.”). The pulsation strain signal was then measured for 5 s after the cuff-type electronic sphygmomanometer completed its operation. Next, the

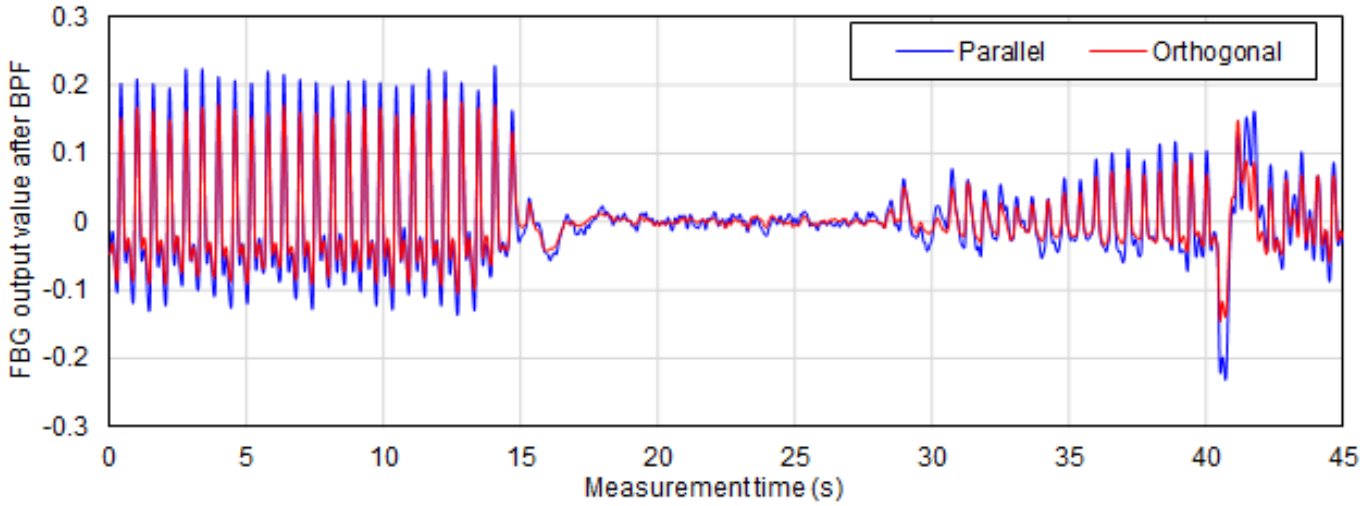

Fig. 4. Signal waveform measured by the FBG sensor during cuff operation (participant C).

pulsation strain signal was measured for approximately 30 s. The signal waveform shape measured during the time the cuff operated and the signal waveform shape before and after operation were verified. In each experiment, data were measured for a total of 25 times, i.e., five times each for five participants.

Fig. 4 shows the signal waveform measured for participant C. The cuff did not operate until the measurement time was 5 s, and therefore, a signal that included a periodic peak was measured. The cuff operated between 5–14 s; however, no tightening pressure was applied to the upper arm. Hence, a periodic signal was detected. The measurement signal waveform changed between 14–17 s when the upper arm was tightened by the cuff. Between 17 and 28 s, the cuff tightened the forearm to the maximum extent. Thus, no peak appeared in the measurement signal. Between 28 and 41 s, the cuff was loosened gradually; hence, it represents the time when blood flow resumes. During this time, small peaks appear continuously. The large baseline fluctuation of the measured signal waveform at the measurement time of approximately 42 s is attributed to the strain when the arm moves because of the opening movement of the cuff. A large peak appears in the measurement signal at 43 s after the cuff operation is completed. Further, this phenomenon appeared in all measurements for each participant. These results indicate that the strain-signal waveform of the fingertip measured by the plastic FBG sensor changes based on the tightening condition of the cuff. That is, the change in the signal waveform is considerably affected by blood-flow conditions. Thus, the measured signal waveform shows a pulsating strain. In addition, the size of the peak of the measurement signal changes depending on the cuff-tightening condition. Therefore, it is believed that the pressure information of the blood flow is included. This blood flow pressure information may help clarify the frequency that is highly related to the reference blood pressure using the length of the vertical axis or the frequency analysis by the Fourier transform. Using the cuff sensor, systolic and diastolic blood pressures can be measured, and the blood flow pressure information can be used as blood pressure. Thus, blood pressure can be calculated from this information, and it may be possible to measure blood pressure at the fingertips easily.

C. Calculation of pulse rate with a plastic FBG sensor system

The calculation of the pulse rate was verified using the signal measured by the plastic FBG sensor. A cuff-type electronic sphygmomanometer was used to measure the reference pulse rate. Similar to previous experiments, the strain signal was measured on the tip of the middle finger using a plastic FBG sensor. The measurement conditions included a measurement time of 10 s and a sampling rate of 1,000 Hz. Subsequently, a cuff-type electronic sphygmomanometer was attached to the forearm of the same arm as the measurement unit, and the reference pulse rate was measured. These two types of measurements were performed in one experiment, and the signal shape and reference pulse rate measured by the plastic FBG sensor were matched. A total of eight participants were part of this experiment (age range: 20–40 years). The data for each participant were measured eight times. The time of all peaks contained in the signal measured by the plastic FBG sensor was measured. The average peak interval time was then calculated for each of the peak time intervals. This peak time interval was divided by 60 to calculate the pulse rate per minute. The calculated pulse rate and reference pulse rate were then verified. The correlation coefficient and calculation accuracy were verified for each of the eight data points measured for each participant to eliminate the influence of individual differences. Then, to verify the versatility, the correlation coefficient and calculation accuracy were verified against a total of 64 data items measured by all participants. The result of the measurement accuracy of the pulse wave number calculation from the signal measured at the fingertip was verified.

Table III summarizes the correlation coefficient and measurement accuracy of the calculated pulse rate with respect to the reference pulse rate for each participant. The summarized results are displayed as “All.” Fig. 5 shows a correlation scatter plot of the pulse-rate calculation for all participants.

TABLE III
RESULTS OF PULSE RATE CALCULATED FROM PLASTIC FBG SENSOR SIGNAL

Participant	R	Accuracy (bpm)	Ave. Ref. PR (bpm)	Ave. Cal. PR (bpm)
A	0.981	±3.7	91.9	90.6
B	0.950	±4.9	91.4	87.6
C	0.843	±9.2	84.8	82.2
D	0.918	±5.6	80.5	76.3
E	0.875	±5.3	77.5	75.4
F	0.900	±3.8	69.8	71.5
G	0.896	±8.5	71.9	66.1
H	0.892	±2.7	62.8	61.2
All	0.925	±5.5	78.8	76.4

Ave. Ref. PR = Average reference Pulse rate.
Ave. Cal. PR = Average calculation Pulse rate.

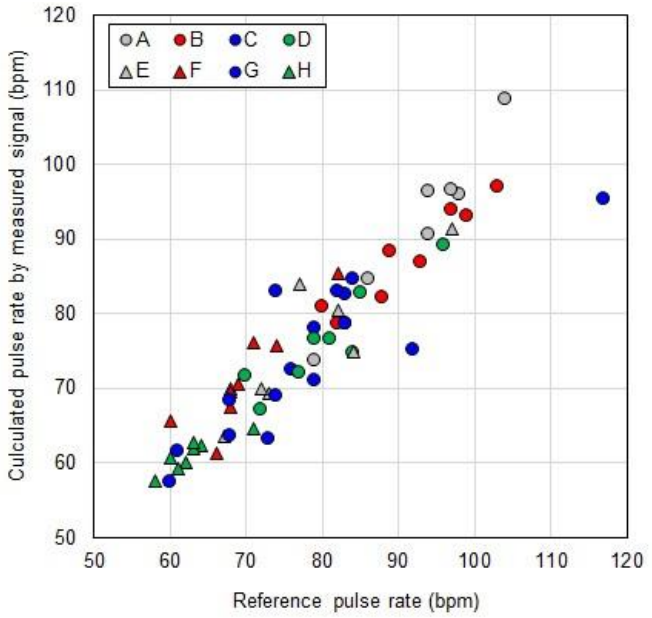

Fig. 5. Correlation scatter plot of reference pulse rate and calculated pulse rate for each participant.

Table III indicates that the correlation coefficient between the pulse rate and reference pulse rate calculated for each participant exceeded 0.8, which suggests a significant correlation. The calculation accuracy ranged between ±2.7–±9.2 bpm. For participants C and G, the calculation accuracy was lower because one of the eight datasets calculated a pulse rate that differed from the reference by approximately 20 bpm. For the other participants, the calculation accuracy was ±5.6 bpm or less, which was approximately 7 % or lower of the average reference pulse wave number of each participant. Among the data of all participants, the correlation coefficient was 0.925, and the calculation accuracy was ±5.5 bpm. These results indicated that the pulse rate was calculated with a high calculation accuracy from the signal obtained by measuring the fingertip with a plastic FBG sensor. One vital sign was measured very easily because the measurement was performed simply by placing the fingertip on the FBG sensor. Furthermore, the measurement time was 10 s; thus, the measurement was possible in a short time.

IV. CONCLUSIONS

In this study, the strain on the fingertip was measured using a plastic FBG sensor, and the following results were obtained.

1) When the plastic FBG sensor was installed at a point 10 or 15 mm from the DIP joint, the strain signal caused by pulsation was measured by all participants, and this measurement point was the narrow arterial blood vessel progressing from the transverse palmar arch to the fingertip direction.
2) The average amplitude length of the measured strain signal did not differ significantly, according to the installation direction of the plastic FBG sensor.
3) When the blood-flow condition was changed by the cuff, the waveform of the signal measured by the FBG sensor also changed, and the pressure information of the blood flow was included.
4) The pulse rate was calculated from the measurement waveform with a measurement accuracy of ±5.5 bpm.

A PPG sensor measures the movement of capillaries; however, the signal measured by the FBG sensor corresponds to changes in the diameter of the artery [14]. More detailed circulatory information can be detected from arterial strain signals measured at various points in the body. Further, if information on arteries throughout the body is detected, new medical methods can be proposed.

The pulsation strain signal can be measured simply by placing the fingertip into a plastic FBG sensor. In this study, the pulse rate was calculated, and the signal waveform measured by the blood flow condition was found to be different. Thus, it was predicted that the measured signal includes the pressure information of the blood flow. Then, the blood pressure can be calculated. The proposed measurement method allows measuring the signal waveform in ~10 s without using a cuff; in addition, it is safe and easy to use for everyone, including children and the elderly. Therefore, pulsation strain measurement using a plastic FBG sensor can help many people.

However, our proposed method has limitations in that the measurement system uses an expensive FBG interrogator, and it is necessary to reduce cost to employ it in everyday life. The high cost is attributed to the use of a plastic FBG sensor. If the pulsation strain can be measured using a silica glass FBG sensor, the cost can be minimized as per the research results reported by other institutions [25]. To this end, a wearable FBG interrogator has been developed; and its use is expanding [26-27]. We plan to determine whether the pulsation strain of the fingertip can be measured with a glass FBG sensor. In addition, in the future, we will develop a method for calculating blood pressure from the measured signal waveform as a future study.

REFERENCES

[1] A. B. Hertzman, "The blood supply of various skin areas as estimated by the photoelectric plethysmograph," *Am. J. Physiol.*, vol. 124, no. 2, pp. 328-340, 1938. [Online]. Available: https://doi.org/10.1152/ajplegacy.1938.124.2.328

[2] A. A. Kamshilin and N. B. Margaryants, "Origin of photoplethysmographic waveform at green light," *Phys. Procedia.*, vol. 86, pp. 72-80, 2017. [Online]. Available: https://doi.org/10.1016/j.phpro.2017.01.024

[3] Y. Meada, M. Sekine, and T. Tamura, "The advantage of wearable green reflected photoplethysmography," *J. Med. Sys.*, vol. 35, no. 5, pp. 829-834, 2011. [Online]. Available: https://doi.org/10.1007/s10916-010-9506-z

[4] E. J. van Kampen and W. G. Zijlstra. (1966). "Determination of hemoglobin and its derivatives," *Adv. Clinic. Chem.*, vol. 8, pp. 141-187, 1966. [Online]. Available: https://doi.org/10.1016/S0065-2423(08)60414-X

[5] H. Ding, Q. Lu, H. Gao, and Z. Peng, "Non-invasive prediction of hemoglobin levels by principal component and back propagation artificial neural network," *Biomed. Optics Expr.*, vol. 5, no. 4, pp. 1145-1152, 2014. [Online]. Available: https://doi.org/10.1364/BOE.5.001145

[6] M. Elgendi, "On the analysis of fingertip photoplethysmogram signals," *Current Cardiol. Rev.*, vol. 8, no. 1, pp. 14-25, 2012. [Online]. Available: https://doi.org/10.2174/157340312801215782

[7] R. R. Anderson and J. A. Parrish, "The optics of human skin," *J. Investig. Dermatol.*, vol. 77, no. 1, pp. 13-19, 1981. [Online]. Available: https://doi.org/10.1111/1523-1747.ep12479191

[8] M. Lemay, M. Bertschi, J. Sola, P. Renevey, J. Parak, and I. Korhonen, "Application of optical heart rate monitoring," in *Wearable Sensors*, Academic Press, 2014, pp. 105-129.

[9] S. Salehizadeh, D. Dao, J. Bolkhovsky, C. Cho, Y. Mendelson, and K. H. Chon, "A novel time-varying spectral filtering algorithm for reconstruction of motion artifact corrupted heart rate signals during intense physical activities using a wearable photoplethysmogram sensor," *Sensors*, vol. 16, no. 1, p. 10, 2015. [Online]. Available: https://doi.org/10.3390/s16010010

[10] S. M. A. Salehizadeh, D. K. Dao, J. W. Chong, D. McManus, C. Darling, Y. Mendelson, K. H. Chon, "Photoplethysmograph signal reconstruction based on a novel motion artifact detection-reduction approach. Part II: Motion and noise artifact removal," *Annals Biomed. Eng.*, vol. 42, no. 11., pp. 2251-2263, 2014. [Online]. Available: https://doi.org/10.1007/s10439-014-1030-8

[11] Z. Zhang, Z. Pi, B. Liu, "TROIKA: A general framework for heart rate monitoring using wrist-type photoplethysmographic signals during intensive physical exercise," *IEEE Trans. Biomed. Engin.*, vol. 62, no. 2, pp. 522-531, 2015. [Online]. Available: https://doi.org/10.1109/TBME.2014.2359372

[12] T. Shimazaki, S. Hara, H. Okuhata, H. Nakamura, and T. Kawabata, "Motion artifact cancellation and outlier rejection for clip-type ppg-based heart rate sensor," In *37th Annual Int. Conf. IEEE EMBC*, 2015, pp. 2026-2029.

[13] S. Koyama, T. Hayase, S. Miyauchi, A. Shirai, S. Chino, Y. Haseda, and H. Ishizawa, "Influence on measurement signal by pressure and viscosity changes of fluid and installation condition of FBG sensor using blood flow simulation model," *IEEE Sensors J.*, vol. 19, no. 24, pp. 11946-11954, 2019. [Online]. Available: https://doi.org/10.1109/JSEN.2019.2938243

[14] S. Miyauchi, T. Hayase, K. Inoue, T. Ogasawara, T. Tsuboi, A. Shirai, S. Chino, S. Koyama, and H. Ishizawa, "Elucidation of mechanism of fiber Bragg grating vital sensing by ultrasonic-measurement-integrated simulation: Flow analysis in ultrasound flow phantom," in *Proc. 15th Int. Conf. on Flow Dynamics.*, 2018. pp. 602-603.

[15] S. Koyama and H. Ishizawa. "Vital sign measurement using FBG sensor for new wearable sensor development," in *Fiber Optic Sensing -Principle, Measurement and Applications*, 1st ed., Chapter 4, S. K. Liaw, Ed. London, UK.: IntechOpen, 2019, pp. 1-16. [Online]. Available: https://doi.org/10.5772/intechopen.84186

[16] S. Koyama, H. Ishizawa, S. Hosoya, T. Kawamura, and S. Chino, "Stress loading detection method using the FBG sensor for smart textile," *J. Fiber. Sci. Technol.*, vol. 73, no. 11., pp. 276-283, 2017. [Online]. Available: https://doi.org/10.2115/fiberst.2017-0042

[17] S. Koyama, A. Fujimoto, Y. Yasuda, and Y. Satou, "Verification of the propagation range of respiratory strain using signal waveform measured by FBG sensors," *Sensors.*, vol. 20, no. 24, p. 7076, 2020. [Online]. Available: https://doi.org/10.3390/s20247076

[18] S. Koyama, H. Ishizawa, A. Sakaguchi, S. Hosoya, and T. Kawamura, "Influence on calculated blood pressure of measurement posture for the development of wearable vital sign sensors," *J. Sensors.*, 8916596, 2017. [Online]. Available: https://doi.org/10.1155/2017/8916596

[19] S. Koyama, H. Ishizawa, K. Fujimoto, S. Chino, and Y. Kobayashi, "Influence of individual differences on the calculation method for FBG-type blood pressure sensors," *Sensors.*, vol. 17, no. 1, p. 48, 2017. [Online]. Available: https://doi.org/10.3390/s17010048

[20] A.G. Leal-Junior, C.A. Diaz, L.M. Avellar, M.J. Pontes, C. Marques, and A. Frizera, "Polymer optical fiber sensors in healthcare applications: A comprehensive review," *Sensors*, vol. 19, no. 14, p. 3156. https://doi.org/10.3390/s19143156

[21] Y. Haseda, J. Bonefacino, H.Y. Tam, S. Chino, S. Koyama, and H. Ishizawa, "Measurement of pulse wave signals and blood pressure by a plastic optical fiber FBG sensor," *Sensors*, vol. 19, no. 23, pp. 5088, 2019. https://doi.org/10.3390/s19235088

[22] J. Bonefacino, H.Y. Tam, T.S. Glen, X. Cheng, C.F.J. Pun, J. Wang, P.H. Lee, M.L.V. Tse, and S.T. Boles, "Ultra-fast polymer optical fibre Bragg grating inscription for medical devices," *Light: Sci. Appl.*, vol. 7, no. 3, 17161, 2017. [Online]. Available: https://doi.org/10.1038/lsa.2017.161

[23] B. Strauch and W. de Moura, "Arterial system of the fingers," *J. Hand Surg.*, vol. 15, no. 1, pp. 148-154, 1990. [Online]. Available: https://doi.org/ 10.1016/S0363-5023(09)91123-6

[24] Y. Hattori, K. Doi, S. Sakamoto, H. Yamasaki, A. Wahegaonkar, and A. Addosooki, "Fingertip replantation," *J. Hand Surg.*, vol. 32, no. 4, pp. 548-555, 2007. [Online]. Available: https://doi.org/10.1016/j.jhsa.2007.01.019

[25] J. Wang, T. Huang, F. Duan, Q. Cheng, F. Zhang, and X. Qu, "Fast peak-tracking method for FBG reflection spectrum and nonlinear error compensation," *Opt. Lett.*, vol. 45, no. 2, pp. 451-454, 2020. [Online]. Available: https://doi.org/10.1364/OL.380722

[26] C.A.R. Diaz, A.G. Leal-Junior, L. Avellar, P.F.C. Antunes, M.J. Pontes, C.A. Marques, A. Frizera, and M.R.N. Ribeiro, "Perrogator: A portable energy-efficient interrogator for dynamic monitoring of wavelength-based sensors in wearable applications," *Sensors*, vol. 19, no. 13, p. 2962, 2019. [Online]. Available: https://doi.org/10.3390/s19132962

[27] K. Ogawa, S. Koyama, Y. Haseda, K. Fujita, H. Ishizawa, and K. Fujimoto, "Wireless, portable fiber Bragg grating interrogation system employing optical edge filter," *Sensors*, vol. 19, no. 14, p. 3222, 2019. [Online]. Available: https://doi.org/10.3390/s19143222

Shouhei Koyama (M'17) and received the B.Eng. and M.Eng. degrees in textile science and engineering from the Shinshu University, Nagano, Japan, in 2003 and 2005, and the Ph.D. degree in instrumentation and measurement technology from Shinshu University in 2012.

From 2005 to 2015, he was Technical staff with the Faculty of Textile Science and Technology, Shinshu University. From 2015 to 2017, he was Assistant Professor with Institute for Fiber Engineering, Shinshu University. Since 2017, he has been an Assistant Professor with the Advanced Textile and Kansei Engineering Department, Shinshu University. His research interests includes the optical fiber measurement application and the textile engineering. He is a member of the Society of Fiber Science and Technology, Japan, the Society of the Instrument and Control Engineers, the Illuminating Engineering Institute of Japan, the Japan Society of Kansei Engineering.

Yuki Haseda received a B.S. and M.S. degrees in engineering in 2019 from Shinshu University, Japan. He has been a doctoral student of the Graduate School of Medicine, Science and Technology, Shinshu University since 2019. His research interest is the optical measurement and biological measurement.

Hiroaki Ishizawa (M'15) received the MSc. degree in 1980 from Tohoku University, Japan, and the Dr. Eng. in 1996 in Instrumentation and Measurement Technology from Shinshu University, Japan. From 1980 to 1982, he was with the Surface Analyzing research group of SHIMADZU, and from 1983 to 2002, was at the Agricultural Research Institute of Nagano as the division head of the research and development. His main research topic in this division was the non-destructive measurement of pesticide residues in agricultural products. In 2002, he was an associate professor, Faculty of Textile Science and Technology, Shinshu University. From 2014, he has been at the present post. His main research interest are optical measurement application such as vital sign sensing system based on Fiber Bragg Grating, non-invasive blood glucose measurement by using spectroscopic method, and application of the spectroscopy (NIRs, IRs, THzs) to measure the content of the textile products.

He is a member of IEEE, the Society of Fiber Science and Technology, Japan, The Society of the Instrumentation and Control Engineers, and so on. He has published 120 papers and over 200 technical proceedings mainly in the field of Instrumentation and measurement methodology, and has 13 patents in the related fields.

Futa Okazaki received a B.S. degree in engineering in 2021 from Shinshu University, Japan. He has been a master student of the Graduate School of Science and Technology, Shinshu University since 2021. His research interests are optical measurement and measurement signal processing.

Julien Bonefacino received the B.S. and M.S. degrees in electronic, electrotechnic and automatism, specialty optoelectronic and microwave, from the University of Montpellier, Montpellier, France, respectively, in 2009 and 2011. He obtained his PhD degree in 2017 from the Photonics Research Centre, Electrical Engineering department, The Hong Kong Polytechnic University, Hong Kong, China, in 2017. Since 2017, he has been a Postdoctoral Fellow with the Electrical Engineering Department, The Hong Kong Polytechnic University, Hong Kong, China.

During his studies, he has worked on the implementation and test of the radio communication board of the student nano-satellite ROBUSTA developed in the University of Montpellier in partnership with the CNES and ESA. From 2011 to 2012, he has been a Research Assistant in the Photonics Research Centre, Electrical Engineering Department, The Hong Kong Polytechnic University. His PhD was supported by the Hong Kong Ph.D. Fellowship Scholarship in 2013.

His research interests include fiber optic sensing in batteries, polymer optical fibers for biomedical applications, fabrication of photosensitive polymer optical fiber, polymer optical fiber Bragg gratings, and material characterization.

Hwa-Yaw Tam (M'86-SM'00) received the B.Sc. and Ph.D. degrees in electrical and electronic engineering from the University of Manchester, Manchester, U.K. From 1989 to 1993, he was with Hirst Research Center, GEC-Marconi Ltd., London, and worked on WDM optical components and systems, and erbium optical fiber amplifiers. He conducted pioneeringworks in optical fiber amplifiers, invented & patented the low-loss splicing technique for erbium-doped fibers, which enhanced the performance of optical amplifiers significantly. Since 1993, he has been in The Hong Kong Polytechnic University (PolyU), where he has been currently working as the Department Head and the Chair Professor of Photonics in the Department of Electrical Engineering, and also the Director of the Photonic Research Centre. He established several world-class research facilities at PolyU, including two fiber-drawing towers for fabrication of photonics crystal fibers and polymer optical fibers, an ultrahigh-speed communication laboratory, and laser platforms for the fabrication of advanced fiber gratings. His current research interests include fabrication of specialty optical silica fibers and polymer fibers, optical fiber communications, and fiber sensor systems based on fiber Bragg gratings and photonic crystal fibers. He has extensive international research collaborations with many universities around the world and is a keynote/invited speaker at more than 40 international conferences. He has a strong R&D collaboration with industry and his team installed many FBG sensing systems, including an FBG-based SHM system for the 610-m Canton Tower in Guangzhou, China, and several condition-monitoring systems for railways in Hong Kong, China mainland, Taiwan, and India.

Currently, his R&D team is building the world's first city-wide fiber-optic sensing network for condition-based monitoring of metro systems in Hong Kong. He received numerous international awards for his inventions, and is the third Prize Winner of the Berthold Leibinger Innovationspreis 2014. Berthold Leibinger Innovationspreis is a biennial event and it is one of the highest remunerated international innovation prizes for laser technology. He is a Fellow of the Optical Society of America and an IEEE Fellow.